Spectrofluorometer Based on Acousto-Optic Tunable Filters for Rapid Scanning and Multicomponent Sample Analyses

Chieu D. Tran* and Ricardo J. Furlan

Department of Chemistry, Marquette University, Milwaukee, Wisconsin 53233

Advantages of the acousto-optic tunable filter (AOTF), namely its ability for fast scanning and multiple-wavelength diffraction, were exploited to develop a novel, all solid-state, nonmoving parts spectrofluorometer. This instrument is based on the use of two AOTFs: one for excitation and the other for emission. The first AOTF was used to specifically diffract white incident light into a specific wavelength(s) for excitation. Depending on the needs, the second AOTF (i.e., the emission AOTF) can be used as either a very fast dispersive device or a polychromator. In the first configuration, the sample was excited by a single-excitation wavelength; the emitted light was analyzed by the emission AOTF, which was scanned very fast. A speed of 4.8 Å was found to be the fastest speed which the AOTF can be scanned with a reasonable S/N and resolution. With this speed, a spectrum of 150 nm can be measured in 312 μs. Faster scanning is possible but, because of the limitation due to the speed of the acoustic wave, may undesiredly lead to degradation in the S/N and spectral resolution. In the second configuration, both AOTFs were used as a polychromator. Several different rf signals were simultaneously applied into the first AOTF to provide multiple-excitation wavelengths. The emission was simultaneously analyzed at several wavelengths by the emission AOTF. With this configuration, the fluorometer can be used for the analysis of multicomponent samples, and the maximum number of components it can analyze is, in principle, $a \times b$, where a and b are the number of excitation and emission wavelengths, respectively. The multicomponent analysis was successfully performed for four component samples using the preliminary setup where $a = b = 2$.

INTRODUCTION

One of the most active research activities in the field of analytical fluorescence spectrometry is instrumentation development for multidimensional measurements. This is because the fluorescence technique, which inherently has ultrasensitivity, has not been widely used for trace characterization of real-time samples. The underutilization stems from the fact that real-time samples normally exist in multicomponent form, and as a consequence, their analyses require measurement of fluorescence at more than one excitation wavelength. Novel development includes instruments which are based on the use of either a photodiode array detector, a vidicon, a charge-coupled device (CCD), or a charge injection device (CID) for multichannel detection.[1-8] With their multidimension capabilities, i.e., the ability to simultaneously measure fluorescence spectra at more than one excitation wavelength, these instruments have proven to be effective for analyses of real-time multicomponent samples.[1-8] Unfortunately, they all suffer from disadvantages such as low sensitivity, high cost, and extensive data acquisition and analysis.[1-8] These limitations are somewhat alleviated in the recently developed fluorometer which is based on the acousto-optic tunable filter.

An acousto-optic tunable filter (AOTF) is an electronic dispersive device.[9-13] It is based on the acousto-optic interaction in an anisotropic medium.[9-13] Acoustic waves, which are applied to the anisotropic crystal though piezoelectric transducers, produce a periodic moving grating which will diffract portions of an incident beam. The conservation of momentum dictates that only a very narrow band of optical frequencies can be diffracted. Therefore, the AOTF will diffract incident white light into a specific wavelength when a specific rf is applied to it. The wavelength of the diffracted light can be tuned over large optical region by simply changing the frequency of the applied rf.[9-13] The diffracted light need not be a monochromatic light. Multiwavelength light can be diffracted from the AOTF when several rf signals are simultaneously applied into the filter.[9,14] In contrast to conventional polychromators, with this electronic AOTF polychromator it is possible to individually amplitude modulate each wavelength of the diffracted multiwavelength light at a different frequency (by individually and sinusoidally modulating each applied rf signal at the desired frequency).[9,14] This feature allows us to develop the first multidimensional fluorometer that is based on the AOTF. In this instrument, the sample was simultaneously excited by two different wavelengths (514.5 and 488.0 nm) whose amplitudes were sinusoidally modulated at two different frequencies (100 and 66 Hz).[14] Two component samples, e.g., mixtures of rhodamine 6G and rhodamine B, were successfully analyzed using this AOTF-based fluorometer.

This AOTF-based fluorometer provides a revolutionary new concept in the field of multidimensional fluorescence

(1) Warner, I. M.; Callis, J. B.; Davidson, E. R.; Gauyeman, M.; Christian, G. D. *Anal. Lett.* **1975**, *8*, 665.
(2) Warner, I. M.; Patonay, G.; Thomas, M. P. *Anal. Chem.* **1985**, *57*, 463A.
(3) Ndou, T. T.; Warner, I. M. *Chem. Rev.* **1991**, *91*, 493.
(4) Warner, I. M.; McGown, L. B. *Advances in Multidimensional Luminescence*; JAI Press, Inc.: Greenwich, CT, 1991.
(5) Vo-Dinh, T. *Room Temperature Phosphorimetry for Chemical Analysis*; John Wiley: New York, 1986.
(6) Warner, I. M.; Callis, J. B.; Christian, G. D.; Davidson, E. R. *Anal. Chem.* **1977**, *49*, 564.
(7) Rossi, T. M.; Warner, I. M. *Appl. Spectrosc.* **1984**, *38*, 422.
(8) Johnson, D. W.; Callis, J. B.; Christian, G. D. *Anal. Chem.* **1977**, *49*, 747A.
(9) Tran, C. D. *Anal. Chem.* **1992**, *64*, 971A.
(10) Tran, C. D.; Bartelt, M. *Rev. Sci. Instrum.* **1992**, *63*, 2932.
(11) Tran, C. D.; Furlan, R. J. *Appl. Spectrosc.* **1992**, *46*, 1092.
(12) Tran, C. D.; Simianu, V. *Anal. Chem.* **1992**, *64*, 1419.
(13) Treado, P. J.; Levin, I. W.; Lewis, E. N. *Appl. Spectrosc.* **1992**, *46*, 553.
(14) Tran, C. D.; Furlan, R. J. *Anal. Chem.* **1992**, *64*, 2775.

0003-2700/93/0365-1675$04.00/0

spectrometry and is effectively used for analyses of multicomponent samples.[14] However, its advantages, or rather the advantages of the AOTF, have not been fully utilized. For example, in this instrument the AOTF is placed in the excitation beam to select the excitation wavelengths. The number of components in a sample which the instrument can analyze is limited by (and is equal or less than) the number of the excitation wavelengths. Since this number is defined by the number of the different rf signals which are simultaneously applied to the filter, it is limited by the total rf power which the filter can tolerate. Generally, AOTFs can tolerate a total rf power of a few watts, and it normally requires at least several hundred milliwatts of power of each applied rf signal to achieve reasonable diffraction efficiency. The total number of wavelengths of light an AOTF can simultaneously diffract is, therefore, limited to ~10. As a consequence, it would be difficult for this AOTF-based fluorometer to analyze samples which have more than 10 components. This limitation can be eliminated, and the number of components in a sample which the fluorometer can analyze can be substantially enhanced, when instead of one, two AOTFs are used: one to disperse the excitation wavelengths and the other to disperse the emission wavelengths. This is because for a sample which has no spectral overlap among its components, the number of components such an instrument can analyze is theoretically equal to $a \times b$, where a is the number of excitation wavelengths and b is the number of emission wavelengths. Therefore, in principle, such an instrument can analyze a sample containing up to 100 different components (it should be realized that, in reality, the number of analyzing components may be less if there are large differences in the fluorescence quantum yields of the components and/or there is extensive spectral overlap among them[8]).

In addition to such advantages as compact, all solid state, wide angular field, high throughput, wide tuning range, high spectral resolution, and high speed random or sequential wavelength access, the AOTF also can be spectrally scanned at high speed. This is because light is diffracted from the AOTF by the acoustic waves.[9] The scanning speed of the AOTF is, therefore, controlled by the transit time of an acoustic wave across an optical beam, which in this case is on the order of a few microseconds.[9] As a consequence, the tuning speed of the filter can be as fast as a few microseconds. However, this fast scanning ability of the AOTF has not been exploited in the reported fluorometer.[14]

Such considerations prompted us to develop a new fluorometer which employs two AOTFs: one to select the excitation wavelengths and the other to disperse the emission wavelengths. In addition to the instrumentation development, experiments will be systematically designed to demonstrate the full advantages of this fluorometer, namely, the ability of the instrument to provide information on the identity of the sample by its ability to provide a quick scan (microseconds) of the emission spectrum of the sample. It will also be demonstrated, using actual samples containing mixtures of dyes, that quantitatively this fluorometer is capable of analyzing multicomponent samples, and the maximum number of components the instrument can analyze equals $a \times b$, where a and b are the number of excitation and emission wavelengths, respectively.

THEORY

It is known that the AOTF will diffract light of one specific wavelength λ_n when a rf signal of rf_n is applied into it. When this rf signal is sinusoidally modulated, the diffracted light is also sinusoidally modulated at the same frequency. This is because the modulated rf induces the sinusoidal modulation in the diffraction efficiency of the AOTF. The magnitude of the modulated diffracted light is proportional to the rf power ${P^{rf}}_n$ and to the modulation level M_n of the rf signal.

When the rf signal, which has the power of

$$ {P^{rf}}_n(t) = {P^{rfo}}_n({Mo^{rf}}_n + {M^{rf}}_n \sin(\omega_n t)) \quad (1) $$

is applied into the AOTF, the diffraction efficiency at wavelength λ_n is given by

$$ E_{\lambda n}(t) = {Mo^{ef}}_{\lambda n} + {M^{ef}}_{\lambda n} \sin(\omega_n t) \quad (2) $$

where ${Mo^{ef}}_{\lambda n}$ is proportional to ${P^{rfo}}_n{Mo^{rf}}_n$ and ${M^{ef}}_{\lambda n}$ is proportional to ${P^{rfo}}_n{M^{rf}}_n$. The intensity of the diffracted light is

$$ {I^{D}}_{\lambda n}(t) = I_{\lambda n}(t)E_{\lambda n}(t) \quad (3) $$

where $I_{\lambda n}(t)$ is the intensity of the incident light at λ_n.

When an unmodulated continuous light source is used, $I_{\lambda n}(t)$ is equal to a constant $Io_{\lambda n}$ and as a consequence, the diffracted light is only modulated at frequency ω_{d_n}:

$$ {I^{d}}_{\lambda n}(t) = {Mo^{d}}_{\lambda n} + {M^{d}}_{\lambda n} \sin(\omega_{d_n} t) \quad (4) $$

where ${Mo^{d}}_{\lambda n} = Io_{\lambda n}{Mo^{ef}}_{\lambda n}$ and ${M^{d}}_{\lambda n} = Io_{\lambda n}{M^{ef}}_{\lambda n}$.

The incident beam can also be sinusoidally modulated with frequency ${\omega^{inc}}_{\lambda n}$, as in the case of the light diffracted from an AOTF which is modulated at a frequency of ${\omega^{inc}}_{\lambda n}$ and has diffraction efficiencies of

$$ {Mo^{inc}}_{\lambda n} = {Io^{inc}}_{\lambda n}{Mo^{ef1}}_{\lambda n} $$

$$ {M^{inc}}_{\lambda n} = {Io^{inc}}_{\lambda n}{M^{ef1}}_{\lambda n} $$

The intensity of the incident light in this case is

$$ {I^{inc}}_{\lambda n}(t) = {Mo^{inc}}_{\lambda n} + {M^{inc}}_{\lambda n} \sin({\omega^{inc}}_{\lambda n} t) \quad (5) $$

This incident light, ${I^{inc}}_{\lambda n}(t)$, when diffracted by a second AOTF which has diffraction efficiencies of ${Mo^{ef2}}_{\lambda 1}$ and ${M^{ef2}}_{\lambda 1}$, and is modulated at a frequency of ω_1, will be a product of eq 4 and eq 5, i.e.,

$$ \begin{aligned} {I^{D}}_{\lambda 1 \lambda n}(t) = {Mo^{D}}_{\lambda 1 \lambda n} + {M1^{D}}_{\lambda 1 \lambda n} \sin({\omega^{inc}}_n t) + \\ {M2^{D}}_{\lambda 1 \lambda n} \sin(\omega_1 t) + {M3^{D}}_{\lambda 1 \lambda n} \cos(({\omega^{inc}}_n - \omega_1)t) + \\ {M4^{D}}_{\lambda 1 \lambda n} \cos(({\omega^{inc}}_n + \omega_1)t) \end{aligned} \quad (6) $$

where

$$ {Mo^{D}}_{\lambda 1 \lambda n} = {Mo^{inc}}_{\lambda n}{Mo^{ef2}}_{\lambda 1} = {Io^{inc}}_{\lambda n}{Mo^{ef1}}_{\lambda n}{Mo^{ef2}}_{\lambda 1} $$

$$ {M1^{D}}_{\lambda 1 \lambda n} = {Mo^{inc}}_{\lambda n}{Mo^{ef2}}_{\lambda 1} = {Io^{inc}}_{\lambda n}{Mo^{ef1}}_{\lambda n}{Mo^{ef2}}_{\lambda 1} $$

$$ {M2^{D}}_{\lambda 1 \lambda n} = {Mo^{inc}}_{\lambda n}{M^{ef2}}_{\lambda 1} = {Io^{inc}}_{\lambda n}{Mo^{ef1}}_{\lambda n}{M^{ef2}}_{\lambda 1} $$

$$ {M3^{D}}_{\lambda 1 \lambda n} = {M^{inc}}_{\lambda n}{M^{ef2}}_{\lambda 1}/2 = {Io^{inc}}_{\lambda n}{M^{ef1}}_{\lambda n}{M^{ef2}}_{\lambda 1}/2 $$

$$ {M4^{D}}_{\lambda 1 \lambda n} = {M^{inc}}_{\lambda n}{M^{ef2}}_{\lambda 1}/2 = {Io^{inc}}_{\lambda n}{M^{ef1}}_{\lambda n}{M^{ef2}}_{\lambda 1}/2 $$

In this work, the fluorescent light emitted by the sample is defined as

$$ L_{\lambda 1 \lambda n}(t) = {I^{inc}}_{\lambda n}(t)F_{\lambda 1}A_{\lambda n} \quad (7) $$

where $L_{\lambda 1 \lambda n}(t)$ is the intensity of the fluorescent light at λ_1 when the sample is excited by λ_n, ${I^{inc}}_{\lambda n}(t)$ is the intensity of the incident beam at λ_n, $F_{\lambda 1}(t)$ is the fluorescence quantum efficiency at λ_1, and $A_{\lambda n}(t)$ is the absorption of the sample at λ_n.

If the excitation light is sinusoidally modulated as in eq 5, the fluorescence light is also modulated; i.e., the whole fluorescence spectrum, not just a single wavelength, is modulated.

A second AOTF is now used to select (i.e., to specifically diffract) the emitted (by excitation at λ_n) fluorescence at λ_1. The intensity of the light diffracted from this second AOTF is given by

$$I^{out}{}_{\lambda 1\lambda n}(t) = F_1 A_n I^{inc}{}_{\lambda n}(t) E_{\lambda 1}(t) \quad (8)$$

which is equivalent to

$$I^{out}{}_{\lambda 1\lambda n}(t) = F_1 A_n I^{D}{}_{\lambda 1\lambda n}(t)$$

$$I^{out}{}_{\lambda 1\lambda n}(t) = F_1 A_n [Mo^{D}{}_{\lambda 1\lambda n} + M1^{D}{}_{\lambda 1\lambda n} \sin(\omega^{inc}{}_n t) + M2^{D}{}_{\lambda 1\lambda n} \sin(\omega_1 t) + M3^{D}{}_{\lambda 1\lambda n} \cos((\omega^{inc}{}_n - \omega_1)t) + M4^{D}{}_{\lambda 1\lambda n} \cos((\omega^{inc}{}_n + \omega_1)t)] \quad (9)$$

The diffracted light, $I^{out}{}_{\lambda 1\lambda n}(t)$, is modulated at five different frequencies, namely 0, $\omega^{inc}{}_n$, ω_1, $\omega^{inc}{}_n - \omega_1$, and $\omega^{inc}{}_n + \omega_1$. In order to deconvolute this signal into five parts that correspond to each frequency, the following integration is performed:

$$\frac{2}{T}\int_T ([I^{out}{}_{\lambda 1\lambda n}(t) \sin(\omega_k t)]^2 + [I^{out}{}_{\lambda 1\lambda i}(t) \cos(\omega_k t)]^2)^{1/2} dt = M^{out}{}_k \quad (10)$$

where T is a period common to all frequencies and $M^{out}{}_k$ is part of the output signal $I^{out}{}_{\lambda 1\lambda n}(t)$ which corresponds to the modulation frequency ω_k, i.e., when

$$\omega_k = 0 \quad \text{then} \quad M^{out}{}_k = Mo_{\lambda 1\lambda n} F_1 A_n$$

$$\omega_k = \omega^{inc}{}_n \quad \text{then} \quad M^{out}{}_k = M1^{D}{}_{\lambda 1\lambda n} F_1 A_n$$

$$\omega_k = \omega_1 \quad \text{then} \quad M^{out}{}_k = M2^{D}{}_{\lambda 1\lambda n} F_1 A_n$$

$$\omega_k = \omega^{inc}{}_n - \omega_1 \quad \text{then} \quad M^{out}{}_k = M3^{D}{}_{\lambda 1\lambda n} F_1 A_n$$

and

$$\omega_k = \omega^{inc}{}_n + \omega_1 \quad \text{then} \quad M^{out}{}_k = M4^{D}{}_{\lambda 1\lambda n} F_1 A_n$$

In principle, the relationship between the measured $M^{out}{}_k$ and the absorption (A_n) and the fluorescence (F_1), i.e.

$$M^{out}{}_k = M3^{D}{}_{\lambda 1\lambda n} F_1 A_n \quad (11)$$

can be used to determine the sample concentration. It is, however, not practical since the intensity of the excitation light $Io^{inc}{}_{\lambda n}$ is not constant but changes with time at the low-frequency region. As a consequence, $M3^{D}{}_{\lambda 1\lambda n}$ also changes with the time, i.e.

$$M3^{D}{}_{\lambda 1\lambda n}(t) = M^{inc}{}_{\lambda n}(t) M^{ef2}{}_{\lambda 1}/2 = Io^{inc}{}_{\lambda n}(t) M^{ef1}{}_{\lambda n} M^{ef2}{}_{\lambda 1}/2 \quad (12)$$

The error due to the fluctuation in the excitation light can be eliminated by initially monitoring the intensity of light incident into the sample $I^{inc}{}_{\lambda n}(t)$ and subsequently performing an integration similar to that in eq 10 for $I^{inc}{}_{\lambda n}(t)$ at $\omega_k = \omega^{inc}{}_{\lambda n}$. This integration will give $M^{inc}{}_{\lambda n}(t)$:

$$M^{inc}{}_{\lambda n}(t) = Io^{inc}{}_{\lambda n}(t) M^{ef1}{}_{\lambda n}/2 \quad (13)$$

The measured fluorescence value of $M3^{D}{}_{\lambda 1\lambda n}(t)$ is then divided by $M^{inc}{}_{\lambda n}(t)$ to give

$$R_{\lambda 1\lambda n} = M^{ef2}{}_{\lambda n} F_1 A_n \quad (14)$$

It is clear from this equation that the measured quantity $R_{\lambda 1\lambda n}$ is proportional to the absorbance and the fluorescence of the sample and is independent of the intensity of the excitation light.

The same treatment can be used for any combination of incident and emission light. If N_i is the number of excitation wavelengths and N_e is the number of emission wavelengths, there will be $N_i \times N_e$ possibilities, and as a consequence, the AOTF-based fluorometer can be used for the analysis of a sample having up to $N_i \times N_e$ components. In this case, a $R_{\lambda 1\lambda n}$ calibration curve for each component is constructed, and the concentrations of each component in the sample can be calculated by solving a matrix of equations.

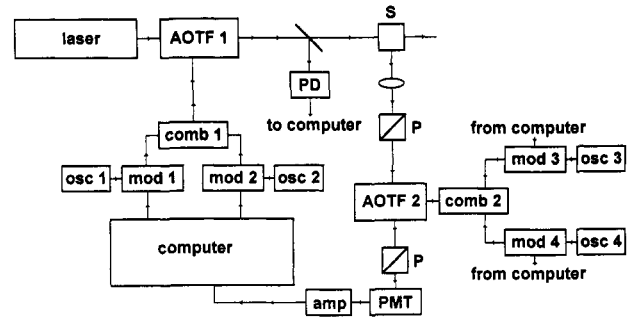

Figure 1. Schematic diagram of the AOTF-based fluorometer: AOTF, acousto-optic tunable filter; PD, PIN photodiode; S, sample; P, polarizer; PMT, photomultiplier tube; amp, amplifier; osc, oscillator; mod, modulator; comb, combiner.

EXPERIMENTAL SECTION

A schematic diagram of the fluorometer based on acousto-optic tunable filters is shown in Figure 1. An argon ion laser (Spectra-Physics Model 165) was used as the excitation source. When operated in the multiline mode, this laser provided output radiation which is a combination of six different colors: 457.9, 476.5, 488.0, 496.5, 501.7, and 514.5 nm. A noncolinear AOTF fabricated from TeO_2 (AOTF 1, Brimrose Corp., Baltimore, MD; Model TEAF-40-70H) was used to select the appropriate excitation wavelength(s). Depending on the type of measurement, this AOTF was driven by either one or two (different) rf signals. Two oscillators (osc 1 and osc 2, MCM Electronics Centerville, OH; Model TENMAC 72-585) were used to supply two rf signals. These two rf's were amplified and sinusoidally modulated by use of home-built devices (mod 1 and mod 2) whose electronic circuitries are the same as the ones used in our previous work.[14] The modulated rf signals were then combined by a combiner (comb 1; Mini-Circuits splitter/combiner Model ZSC-2-1). Before being connected to the AOTF this combined signal was amplified one more time by means of a Mini-Circuits high-power amplifier (Model ZHL-1-2W). This amplification process was necessary because in contrast to the Matsushita AOTF used in the previous work,[14] this Brimrose AOTF requires rf signals whose power is in the range of hundreds of milliwatts. The amplified, modulated signal was then applied onto the AOTF to enable it to diffract the incoming multiline laser beam into a beam which has specific wavelength(s). The intensity of the diffracted light was adjusted to be the same for all excitation wavelengths. This was accomplished by appropriately controlling the power of the applied rf signals. To do this, a small portion of the diffracted light was split by means of a beam splitter and detected by a reference photodiode (PD; United Detector Technology, PIN 10 DP). The output of the photodiode was amplified and connected to the microcomputer (IBM compatible with a 486 microprocessor; Milwaukee PC, Milwaukee, WI). A major portion of the light diffracted from the AOTF was used to excite the sample. The fluorescence emitted from the sample was focused onto the second AOTF (i.e., AOTF 2), at 90° in relation to the excitation beam, by means of a lens with a 10-mm focal length. This second AOTF, which is also a noncollinear type TeO_2 AOTF (Matsushita Electronic Components Co., Ltd., Osaka, Japan; Model EFL-F20), was used to spectrally analyze the fluorescence. Three different driver systems were developed to drive this AOTF. The first driver was specifically designed for measurement of the fluorescence spectrum of the sample in the fast time scale (microseconds). It is based on a voltage control oscillator (VCO; Inrad Northvale, NJ, Model 075A010). It is known that the frequency of the rf signal (f_{out}), generated by the VCO is

approximately proportional to the signal applied to it (V_{in}):

$$f_{out} = AV_{in} + B \quad (15)$$

where A and B are constants. In this case, the VCO was driven by a sawtooth signal produced by a function generator. Data acquisition was accomplished by use of a digital oscilloscope (Hewlett-Packard Model 54600A). The oscilloscope was triggered by the same sawtooth signal. The triggering level and the period of the sawtooth signal were adjusted to give a positive slope ramp signal on the oscilloscope. These experimental conditions enable the ramp signal to be

$$V_{in} = Ct + D \quad (16)$$

where C and D are constants. As a consequence of this linear relationship, the frequency of the rf signal generated by the VCO will have the form

$$f_{out} = ACt + E \quad (17)$$

where $E = AD + B$ and is a constant.

The second driver was also developed for measurement of the fluorescence spectrum of the sample. It is based on an inexpensive but highly accurate high-performance frequency generator module equipped with programmable dividers (IC Designs, Kirkland, WA, Model f2PC). Because this device is based on the phase lock loop,[15] the frequency of the output signal (f_{out}) can be set at any value. That is f_{out} is given by

$$f_{out} = (f_{D2}/f_{D1})f_{ref} \quad (18)$$

where f_{D1} and f_{D2} are the frequencies of the reference and the output dividers, respectively, and were supplied by a computer, and f_{ref} is the reference frequency supplied by a crystal. As will be described in the Results and Discussion section, the scanning speed of this driver is relatively slower than the VCO. It has, however, other advantages such as cost effectiveness, precision, accuracy, and ease of use.

The third driver system was designed specifically for multicomponent sample analyses. It is based on the use of two different oscillators to simultaneously apply two different rf's to the AOTF. The electronic configuration and circuitry for this driver is similar to the driver system used to drive the excitation AOTF.

The fluorescence light diffracted from the emission AOTF was separated from the transmitted light by means of polarization. Specifically, a polarizer was placed after the sample and in front of the AOTF to convert the fluorescence light into vertical polarization. Since the polarization of the light diffracted from the AOTF is perpendicular to that of the incident (and also of the transmitted) light, a second polarizer, whose axis is perpendicular to that of the first polarizer, was placed after the AOTF to transmit the diffracted beam and block the transmitted beam. The intensity of the beam emerging from the second polarizer was detected by a photomultiplier tube (PMT; Hamamatsu Model R446) and amplified by an amplifier (amp) prior to being connected to the computer through the A/D of the 12-bit DAS 16 board (Metra-Byte, Taunton, MA).

RESULTS AND DISCUSSION

The fluorescence spectrum of an ethanolic solution of 1.0×10^{-6} M eosin is shown in Figure 2a. This spectrum was obtained by exciting the compound at 514.5 nm and scanning the emission AOTF. The voltage control oscillator (VCO) was used to drive the AOTF so that the fast-scan ability of the filter can be demonstrated. The dispersed fluorescence light was detected by the photomultiplier tube and recorded as a single trace by a digital oscilloscope. The spectrum was initially recorded as the fluorescence intensity versus time. The time was then converted into the acoustic frequencies, f_{out}, by use of eq 17. While it is known that f_{out} is not linearly related to the wavelength of the diffracted light[9] it can be

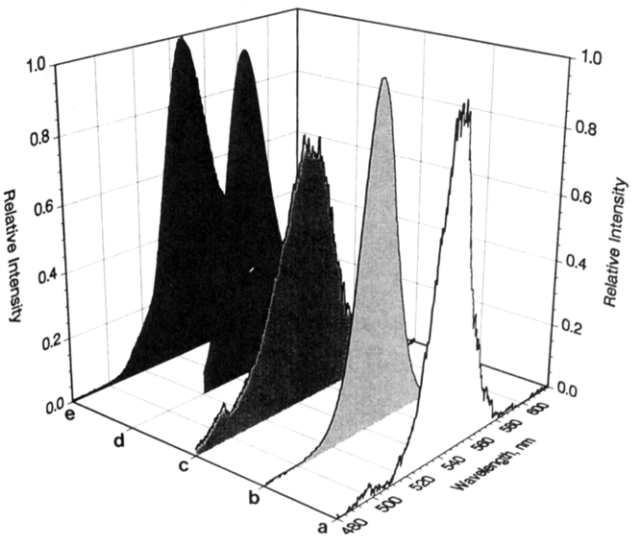

Figure 2. Fluorescence spectra of 1.0×10^{-6} M eosin in ethanol: (a) AOTF2 at a scanning rate of 4.8 Å/μs; (b) an average of 256 spectra taken at the same scanning rate as in (a); (c) AOTF2 at a scanning rate of 12.4 Å/μs; (d) Perkin-Elmer spectrofluorometer; (e) AOTF2 at a very slow scanning rate.

approximately assumed, under the narrow spectral range used in this work (about 150 nm), to have a linear relationship of

$$\lambda = [V_a(n_e - n_o)]/f_{out} \quad (19)$$

where v_a is the acoustic frequency in the AOTF, i.e., TeO_2, and is reported to be to 6.17×10^2 m/s;[16] n_e and n_o are the refractive indices of the extraordinary and ordinary light in TeO_2, respectively.[17] To facilitate the conversion a calibration was made in which the scattering of the excitation light at 476.5 and 514.5 nm was measured by means of a scattering solution (aqueous suspension of talc).

Conditions under which the fluorescence spectrum shown in Figure 2a was taken correspond to a scanning speed of 38 nm/79 μs (i.e., 4.8 Å/μs). Since the fluorescence spectral bandwidth of this compound is on the order of 150 nm it takes ~312 μs to measure one fluorescence spectrum for each compound. As illustrated, the S/N of this spectrum is rather poor. Improvement in the S/N can be easily accomplished by signal averaging. Shown in Figure 2b is the average of 256 spectra taken at conditions identical to that in (2a) (i.e., at a scanning rate of 4.8 Å/μs). The S/N of this averaged spectrum was substantially improved compared to that of the single spectrum (2a). The S/N enhancement, calculated as the ratio of the rms of the averaged signal (2b) to that of the signal (2a), was found to be 12.5. This value is relatively smaller than the $(256)^{1/2}\times = 16\times$ enhancement, which was expected from the signal averaging. A variety of reasons might account for this discrepancy, including the noise from the eight-bit oscilloscope used to record signals.

In principle, a scanning speed of 4.8 Å/μs is not the fastest speed at which we can scan this AOTF-based instrument. The VCO can be scanned as quickly as 10 μs, and the response times for the PMT and its amplifier are on the order of nanoseconds. The limiting factor is, therefore, on the AOTF, i.e., the transit time of the acoustic wave across the optical beam. As described above, the speed of an acoustic wave in TeO_2 is equal to 6.17×10^2 m/s.[15] It is estimated that it will take ~14.2 μs for an acoustic wave to travel across the AOTF used in this work. As a consequence, the scanning speed of the system can, in principle, be much faster. To demonstrate this, we measured the fluorescence spectra of the same eosin

(15) Horowitz, P.; Hill, W. *The Art of Electronics*; Cambridge University Press: New York, 1983.

(16) Sapriel, J. *Acousto-Optics*; John Wiley: New York, 1976.

(17) Brimrose Corp., Baltimore, MD, personal communication, 1992.

solution at scanning speeds of 12.4 Å/μs and the spectrum obtained is shown in Figure 2c. As depicted, the spectrum in this case is different from the one shown in (2a). The spectrum shown in (2c) is wider and has a smaller magnitude than those in (2a) and (2b). For reference, fluorescence of the same eosin solution taken with a Perkin-Elmer LS 5 spectrofluorometer is shown in Figure 2d. This steady-state spectrum is similar to the spectrum shown in (2a) and in (2b) and is different from that in (2c). It is evidently clear that faster scanning speed led not only to lower S/N but also to the distortion of the spectrum. The distortion in (2c) is due to the degrading in the resolution of the AOTF by the fast scanning. That is when the scanning is fast, there are more than one acoustic waves present in the filter. As a consequence, there will be overlap between the residual and the incoming acoustic waves and the diffraction of the light in this region suffers degradation in the resolution. Without detailed information on the construction and dimension of the AOTF, it is difficult to precisely calculate the effect of scanning speed on the resolution of the AOTF. Furthermore, the resolution of the filter is also dependent on the characteristics of the incident light, namely, the monochromaticity and the collimation of the light. It can be assumed, by a very rough approximation, that the degradation in the resolution of the AOTF is directly proportional to the scanning speed and the time it takes for the acoustic wave to travel across the filter. With this approximation, it can be calculated that increasing the scanning speed from 4.8 to 12.4 Å/μs led to a 10.8-nm degradation in the resolution of the filter. This value agrees relatively well with the results obtained in this work.

Taken together, the results obtained seem to indicate that the fastest speed which this AOTF-based fluorometer can be scanned without much compromise in the resolution is 4.8 Å/μs. Of course, the S/N will not be high when the spectrum is taken at this high speed. However, as demonstrated in Figure 2b, the low S/N can easily be overcome by signal averaging. It is important to add that, at this scanning speed, even with the averaging of 256 signals, the total time required to acquire the spectrum shown in (2b) was only 80 ms.

When fast scanning is not required, it is more accurate and economical to drive the AOTF with a rf generator (digital) board rather than a VCO. In this case, because the rf frequency was digitally generated by a computer, it is very precise and accurate. Direct knowledge of the rf frequency made it relatively easier to convert to the wavelength of the diffracted light and, as a consequence, made it possible to accurately determine the exact wavelength of the diffracted light at any point during the scan. There are no complications as in the case of the VCO where the applied voltage was initially converted to the rf frequency (where the conversion factor is not strictly linear over a wide range) before being changed to the wavelength of the diffracted light. The only disadvantage of the particular (economical) rf board used in this work is its limited scanning speed. Specifically, the fastest speed which this board can scan is 20 ms. As a consequence, it takes ~22 s to scan over 150 nm at a scan of 5 points/nm. Figure 2e shows the fluorescence spectrum of the eosin solution taken when the AOTF was driven by the rf digital board at such a scanning rate. As illustrated, the spectrum in this case has high resolution and is the same as the steady-state spectrum taken with the Perkin-Elmer fluorometer (2c). Of course, it is possible to measure the spectrum at a faster scanning rate (and at lower resolution) by taking a fewer number of points; e.g., when only 1 point/nm was used, the time it took to measure the spectrum was only 4.4 s.

All fluorescence spectra shown in Figure 2 were taken when the eosin solution was excited at 514.5 nm. Spectra can also be taken at other excitation wavelengths by simply changing

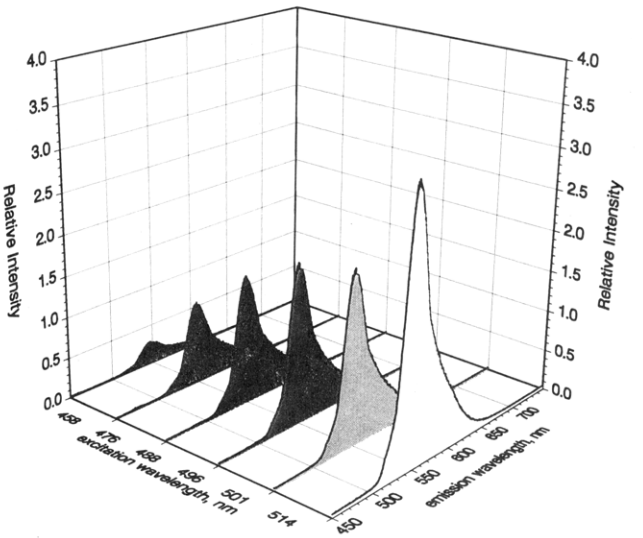

Figure 3. Fluorescence spectra of 1.0×10^{-6} M eosin in ethanol taken at different excitation wavelengths.

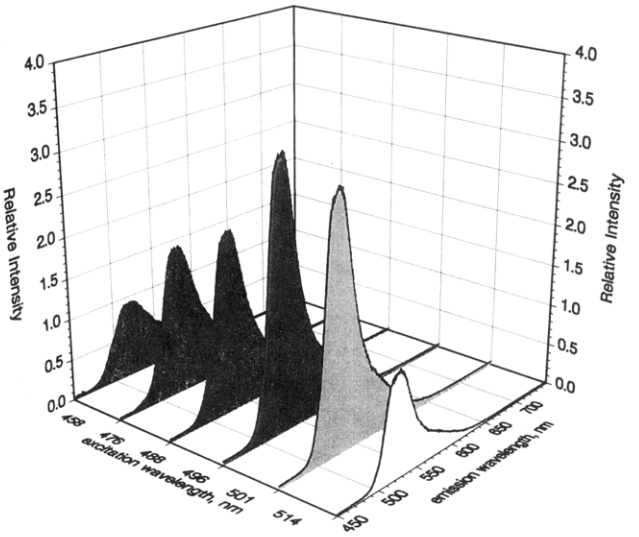

Figure 4. Fluorescence spectra of 1.0×10^{-6} M fluorescein in ethanol taken at different excitation wavelengths.

the frequency of the rf signal applied to the excitation AOTF (i.e., AOTF1). This, in turn, changes the wavelength of the diffracted light. Because, in this work, an argon ion laser operated in the multiline mode was used as the excitation source, there were only six discrete wavelengths available for excitation, 514.5, 501.7, 496.5, 488.0, 476.5, and 457.9 nm. The applied rf frequencies corresponding to these wavelengths were 131.308, 135.965, 137.900, 141.400, 146.300, and 155.210 Mhz, respectively. Shown in Figure 3 are the fluorescence spectra of 1.0×10^{-6} M eosin taken when the sample was excited by each of these excitation wavelengths. In order to achieve high resolution for the spectra, the emission AOTF2 was scanned with the digital rf board driver. The fluorescence spectra of other compounds used, namely, 1.0×10^{-6} M ethanolic solutions of fluorescein, rhodamine B, and 4-(dicyanomethylene)-2-methyl-6-[*p*-(dimethylamino)styryl]-4-*H*-pyran (DMP), are also shown in Figures 4–6, respectively.

Multicomponent sample analysis was performed by mixing these four dyes at various combinations of concentrations. Since these mixtures had four different components two different excitation wavelengths and two emission wavelengths were required for the analysis. These wavelengths were selected at such values where these four molecules have relatively large differences in absorption and emission. The wavelengths were found to be 488.0 and 514.5 nm for excitation

Table I. Simultaneous Determination of Rhodamine B, Fluorescein, DMP, and Eosin by AOTF-Based Fluorescence Spectrometry

	added concn, $\times 10^7$ M				found concn, $\times 10^7$ M							
					rhodamine B		fluorescein		DMP		eosin	
mixture	rhodamine B	fluorescein	DMP	eosin								
1	10.00	10.00	2.00	5.00	10.00	−3%	10.00	−2%	2.00	+5%	5.00	+12%
2	5.00	5.00	4.00	10.00	5.00	+16%	5.00	−2%	4.00	+5%	10.00	+4%
3	5.00	10.00	4.00	5.00	5.00	−4%	10.00	−7%	4.00	+7%	5.00	+2%
4	5.00	5.00	2.00	5.00	5.00	+0%	5.00	−4%	2.00	+0%	5.00	+4%
5	5.00	5.00	1.00	2.50	5.00	+2%	5.00	−2%	1.00	+0%	2.50	−12%
6	2.50	5.00	2.00	2.50	2.50	+0%	5.00	+2%	2.00	+0%	2.50	−12%
7	1.00	1.00	0.80	2.00	1.00	+10%	1.00	+20%	0.80	−12%	2.00	+0%
8	1.00	2.00	0.80	1.00	1.00	−19%	2.00	+5%	0.80	−12%	1.00	+1%
9	1.00	1.00	0.20	0.50	1.00	+0%	1.00	+0%	0.20	+0%	0.50	+0%
10	0.50	1.00	0.40	0.50	0.50	+0%	1.00	+0%	0.40	+0%	0.50	+0%
11	0.50	0.50	0.20	0.50	0.50	−4%	0.50	−2%	0.20	+0%	0.50	+4%

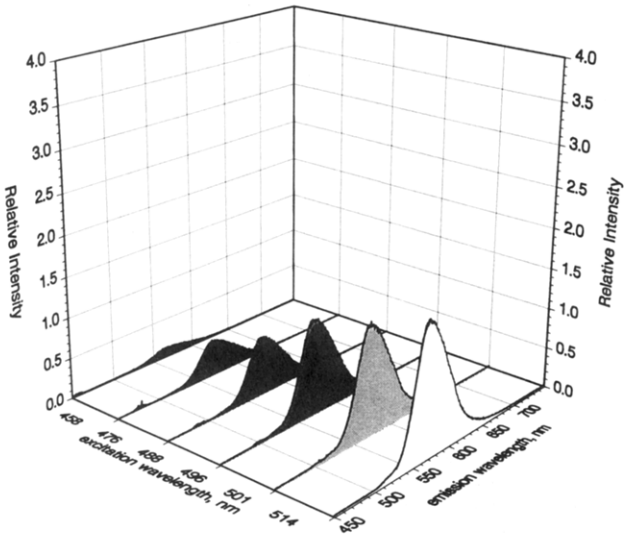

Figure 5. Fluorescence spectra of 1.0×10^{-6} M rhodamine B in ethanol taken at different excitation wavelengths.

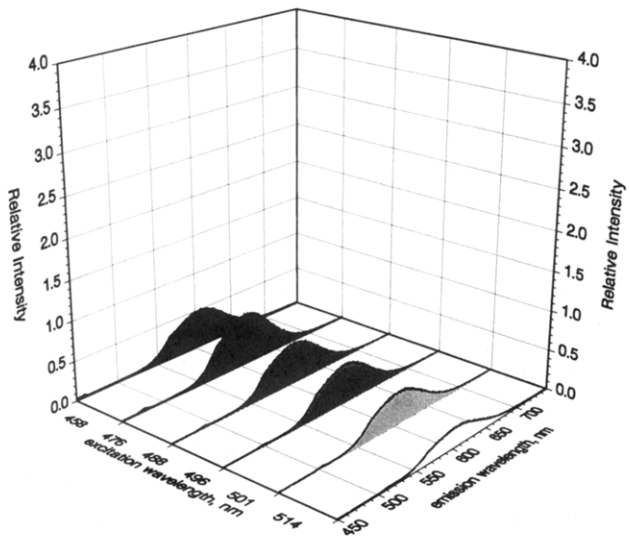

Figure 6. Fluorescence spectra of 1.0×10^{-6} M DMP in ethanol taken at different excitation wavelengths.

and 537.6 and 585.1 nm for emission. To provide these dual excitation wavelengths, two rf signals of 141.400 and 131.308 MHz were simultaneously applied to the excitation AOTF (i.e., AOTF1). The emission AOTF (AOTF2) was driven by the third driver, which is based on the use of two oscillators to simultaneously provide two different rf frequencies at 59.31 and 53.99 MHz. This condition enabled the simultaneous measurement of the fluorescence signal emitted from the sample at 537.6 and 585.1 nm. As described in the Theory section, the concentration of each component in the mixture can only be calculated if each of the four wavelengths is sinusoidally modulated at a different frequency, i.e., ω_1, ω_2, ω_3, and ω_4 for 514.5-, 488.0-, 585.1-, and 537.6-nm beams, respectively. Care must be taken to select these four frequencies in order to avoid overlap not only among them but also among them and their beat frequencies of importance for calculation, i.e., $M3^{D}_{\lambda 1 \lambda n}$ or $\omega_1 - \omega_3$, $\omega_1 - \omega_4$, $\omega_2 - \omega_3$, and $\omega_2 - \omega_4$. It was found that when these four frequencies are a multiple of 15, 16, 20, and 22, respectively, the beat frequencies are a multiple of 4, 5, 6, and 7 and the above conditions are satisfied. Based on these findings, the four sinusoidal modulation frequencies used in this work were selected to be a 136.4, 145.5, 181.8, and 200 Hz for ω_1, ω_2, ω_3, and ω_4, respectively. Using these experimental conditions, calibration curves for the eosin solution were constructed from the fluorescence data obtained when the sample was simultaneously excited at two different excitation wavelengths (488.0 and 514.5 nm, AM modulated at 136.4 and 145.5 Hz, respectively) and detected at two different emission wavelengths (537.6 and 585.1 nm, AM modulated at 181.8 and 200.0 Hz, respectively). Linear relationships (not shown) were obtained for all four cases (correlation coefficients are 0.999 971, 0.999 963 5, 0.999 942 5,and 0.999 926 1) for the concentration range from 1.0×10^{-9} to 1.0×10^{-6} M.

Simultaneous determination of concentrations of each component in the four-component mixture was then performed using this AOTF-based fluorometer. Eleven mixtures were prepared by mixing eosin, fluorescein, rhodamine B, and DMP at different combinations of concentrations. Using the aforementioned experimental conditions and the data analysis method described in the Theory section, the concentrations of each component in the mixtures were calculated from the measured fluorescence intensities at 488.0- and 514.5-nm excitation. The obtained concentrations are listed in Table I together with the added concentrations. In all cases and for concentrations of each component ranging from 2.0×10^{-8} to 1.0×10^{-6} M, good agreement was found between the added concentrations and the calculated values. Relative errors in most cases were only a few percents.

The limit of detection (LOD), defined as the concentration of sample that yielded a signal-to-noise ratio of 2, was estimated for eosin using the aforementioned four calibration curves. The LOD values were found to be 6.69×10^{-10}, 3.47×10^{-10}, 4.0×10^{-10}, and 2.0×10^{-10} M for the four cases, respectively. These LOD values are comparable with LOD values obtained using videofluorometers.[18,19] However, these LOD values were estimated from preliminary results obtained

(18) Johnson, D. W.; Gladden, J. A.; Callis, J. B.; Christian, G. D. *Rev. Sci. Instrum.* **1979**, *50*, 118.
(19) Warner, I. M.; Fogarty, M. P.; Shelly, D. C. *Anal. Chem. Acta* **1979**, *109*, 361.

using the first-generation spectrofluorometer, and this instrument was constructed using optical and electronic components which are available in our laboratory. Further improvement is, therefore, possibly by use of optimal and more appropriate components including polarizers with large angular fields (one of the polarizers used in this work is the Glan-Thompson polarizer, which has a rather small acceptance angle) and a photomultiplier tube with high quantum efficiency (the present PMT is a side-on Hamamatsu R446 tube, which has a rather low quantum efficiency).

Collectively these results clearly demonstrated that a novel, compact, all-solid-state, nonmoving parts, fast-scanning fluorometer can be successfully constructed using acousto-optic tunable filters. The fluorometer not only is capable of measuring a fluorescence spectrum in a time scale as short as microseconds but also can be used for the simultaneous determination of multicomponent samples. In this work, an argon ion laser was used as the excitation source because it is available in our laboratory. The consequence of using this laser is that only six different excitation wavelengths were available, and the number of components which the fluorometer can analyze is limited. However, it is not necessary to use a laser for excitation because, as demonstrated from the present results, particularly that of the diffraction of fluorescence light by the AOTF2, any type of light source including incandescent or arc lamp can be used for excitation. When such light source is used, the number of components in a mixture which this instrument can analyze is limited only the amount of rf power which the AOTFs can tolerate.[9,14] The number of components can, therefore, be as high as hundreds. The possibility is currently under investigation in our laboratory.

ACKNOWLEDGMENT

We are indebted to Mark Bartelt for his competent technical assistance, and to Brimrose Corp for data on Δn values of TeO_2. Acknowledgment is made to the National Institutes of Health, National Center for Research Resources, Biomedical Research Technology Program for financial support of this work.

RECEIVED for review December 28, 1992. Accepted March 22, 1993.